

# Temporal variations in the convective style of planetary mantles

Alexander Loddoch <sup>\*</sup>, Claudia Stein, Ulrich Hansen

*Institute f. Geophysics, Corrensstr. 24, 48149 Muenster, Germany*

Received 30 January 2006; received in revised form 25 August 2006; accepted 25 August 2006

Available online 3 October 2006

Editor: Scott King

## Abstract

Investigations of mantle convection with temperature- and strain-rate-dependent viscosity have shown the existence of fundamentally different convective styles: By varying e.g. the Rayleigh number, the viscosity contrast or the strain-rate dependency of viscosity, the planform of convection in the asymptotic stationary state changes from the so-called stagnant lid regime to an episodic behaviour and further to a state characterised by a permanently mobilised surface. Our studies suggest that this transition may not only be induced by a change of parameters but also occurs temporally for fixed parameters. We have in fact observed convective systems in the stagnant lid regime that show isolated events of surface mobilisation occurring out of a thermally equilibrated state. We use a 3D numerical mantle convection model to investigate mantle convection and surface dynamics as a coupled fluid dynamical system. Our studies focus on the existence of a transitional regime in which temporal variations between the stagnant lid and the episodic regime occur. We were able to deduce a mobilisation criterion that describes the stability of the stagnant surface, thus allowing for a quantitative analysis of the transition to a (temporarily) mobilised surface. This criterion is also suitable to predict the occurrence of surface mobilisation events.

© 2006 Elsevier B.V. All rights reserved.

*Keywords:* mantle convection; convective regimes; episodic regime; stagnant lid; transitional behaviour

## 1. Introduction

Thermal convection is an important mechanism for heat transport in terrestrial planets, with the actual convective style and the thermal evolution differing strongly among the planets. Mars, Mercury and the Moon, for example, are today characterised by an immobile and rigid surface (stagnant lid) under which the convection is confined [1,2]. This behaviour is in contrast to the plate-tectonics style of convection ob-

served on Earth. Here, the rigid surface is actively participating in the convective process, i.e. large surface pieces move from the mid-ocean ridges, where they are newly created by rising material, to subduction zones, where they are pulled into the Earth's interior. While the mobilisation of the surface on Earth is continuous, an occasional mobilisation is found on Venus. Events of resurfacing appear between phases of stagnant lid convection [3–6]. Early episodes of surface mobilisation have also been speculated for Mars but are assumed to have died off today [7–9].

Due to the specific type of surface expression the thermal structure in the planets differ. A thick, conductive lid significantly constrains the heat flux through the surface compared to a mobilised plate that

\* Corresponding author. Fax: +49 251 83 36100.

E-mail addresses: [loddoch@earth.uni-muenster.de](mailto:loddoch@earth.uni-muenster.de) (A. Loddoch), [stein@earth.uni-muenster.de](mailto:stein@earth.uni-muenster.de) (C. Stein), [hansen@earth.uni-muenster.de](mailto:hansen@earth.uni-muenster.de) (U. Hansen).

effectively cools the interior by its sinking. Consequently the interior of planets characterised by the stagnant lid mode of convection is initially heated up [10].

The thermal evolution of terrestrial planets has been widely investigated [e.g. [6,11–15]]. This is commonly done by applying a scaling relationship which comprises a parameterisation of the heat flux in terms of the Rayleigh number. Separate parameterisations have been discussed for different convective regimes by Solomatov [16]. A transition from one convective style to another is thus mimicked by prescribing different scaling laws appropriate for each regime [17].

Several studies using a fully dynamical model have shown that the combination of rheological aspects and mantle convection processes leads to different convective regimes by varying parameters such as the Rayleigh number or rheological parameters [18–20]. For a strongly temperature-dependent viscosity and an increasing strain-rate dependency, these regimes are the stagnant lid regime, the episodic regime and the mobile lid regime.

The stagnant lid regime is dominated by the strong temperature dependence of the viscosity. As such the cold surface material is highly viscous and becomes immobile. Similar to the so-called ‘one-plate’ planets [21] the stagnant lid covers the hot, convecting mantle material.

If the strain-rate dependence of the viscosity also influences the system, the supercritical stresses in the material lead to a reduction of the effective viscosity. As a consequence the surface is weakened and able to move. The sinking of cold surface material and the rising of hot mantle material is comparable to the subduction and accretion of plates on Earth. In the mobile lid regime the surface mobilisation is continuous, while in the episodic regime the convective recycling of the surface material appears repeatedly. In between the stagnant lid recovers almost completely. But due to the fast sequences of mobilisation no thermal equilibrium for the phases of stagnant lid formation is observed.

A further interesting feature occasionally observed, is the temporal variation in the convective styles [18,20]. This has not yet been intensively discussed, though, for example, the change from a previous plate-tectonics style of convection to the stagnant lid mode of convection is of great potential importance for Mars. A further change more relevant for Venus could be the stagnant lid mode of convection interrupted by several, single episodes of surface mobilisation.

The topic of this paper is thus the closer investigation of the transitional behaviour, i.e. the temporal change from the stagnant lid behaviour to (episodic) mobilisation of the surface. A fluid dynamical approach has been applied for this purpose.

## 2. The model

### 2.1. The numerical model

We consider thermally driven convection of an incompressible Boussinesq medium with infinite Prandtl number. The governing equations describing the conservation of mass, momentum and energy, respectively, are as follows:

$$\nabla \cdot \mathbf{u} = 0 \quad (1)$$

$$-\nabla p + \nabla \sigma + Ra T \hat{z} = 0 \quad (2)$$

$$\frac{\partial T}{\partial t} + \nabla(\mathbf{u}T) - \nabla^2 T = Q \quad (3)$$

Here,  $\mathbf{u}$  is the velocity vector,  $p$  the dynamic pressure (i.e. the pressure without the hydrostatic component) and  $\sigma$  the stress tensor with  $\sigma = \eta [(\nabla \mathbf{u}) + (\nabla \mathbf{u})^T]$ .  $T$  is the temperature and  $\hat{z}$  the vertical unit vector. The rate of internal heat production  $Q$  is assumed to be constant in space and time. All variables have been non-dimensionalised by using a common scaling based on thermal diffusion time and vertical temperature difference. The Rayleigh number resulting from this scaling (defined at the surface) reads:

$$Ra = \frac{\alpha \rho g \Delta T d^3}{\kappa \eta_0} \quad (4)$$

where  $\alpha$  denotes the (constant) thermal expansivity,  $\rho$  the density,  $g$  the gravitational acceleration,  $\Delta T$  the vertical temperature difference,  $d$  the height of the model volume and  $\kappa$  the (constant) coefficient of thermal conductivity.  $\eta_0$  is the reference viscosity defined at the surface of the box.

These equations are solved using a numerical method presented by Trompert and Hansen [22]: A finite volume approach is applied for spatial discretisation and an implicit Crank–Nicholson scheme for discretisation in the time domain. The algebraic equations are solved iteratively employing a multigrid technique with SIMPLER as smoother. The experiments were carried out in a Cartesian box with stress-free, impermeable boundaries. The box was heated from below and cooled from above with constant temperatures of  $T_{\text{top}}=0$  and  $T_{\text{bot}}=1$ . Reflecting conditions were employed at the sides.

### 2.2. The rheological model

In order to investigate systems that show variations in the convective style, we employ a viscosity depending on temperature  $T$  and strain-rate  $E$ . This combination

has proven to be suitable to produce both, stagnant lid convection and episodic surface mobilisation, depending on the actual choice of parameters [18,19]. The effective viscosity is calculated as follows:

$$\eta(T, E) = 2 \cdot \left[ \frac{1}{\eta_T} + \frac{1}{\eta_E} \right]^{-1} \quad (5)$$

with

$$\eta_T = \exp(-r \cdot T) \quad \text{and} \quad \eta_E = \eta^* + \frac{\sigma_0}{E} \quad (6)$$

being the temperature- and strain-rate-dependent part of the viscosity, respectively.  $r$  determines the strength of the temperature dependency, with  $R = \exp(r)$  being the viscosity contrast between the material with maximum (i.e.  $T=1$ ) and minimum temperature ( $T=0$ ). All calculations shown in this work have been carried out with  $R=10^5$ .  $\eta^*=10^{-5}$  is the plastic viscosity,  $\sigma_0$  the yield stress and  $E$  the second invariant of the strain-rate tensor.

### 3. Results

The results of previous studies as summarised in the introduction delineate a variation of the convective style as a function of parameters. Planetological considerations as the investigation of the thermal history of Mars or Venus often assume changes in the convective styles occurring as a function of time, for fixed parameters [8,17,23]. Therefore, the question arises, whether such a transition is dynamically plausible and under which circumstances it may occur. Our studies show, that a

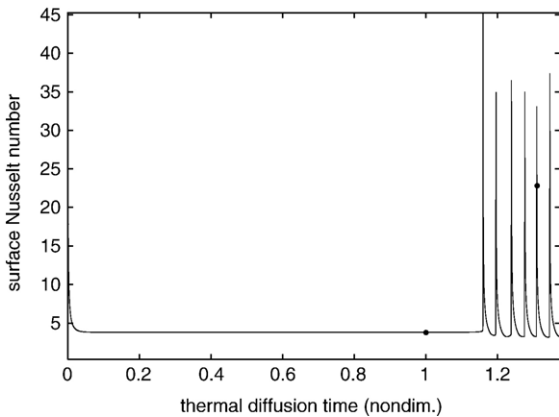


Fig. 1. Surface Nusselt number as a function of time showing a transition from a stagnant lid to an episodic behaviour at  $t=1.16$ . Black dots indicate the points in time of the temperature snapshots in Fig. 2. For this calculation a (surface) Rayleigh number of  $Ra=100$  and a yield stress of  $\sigma_0=1$  have been used (run 1).

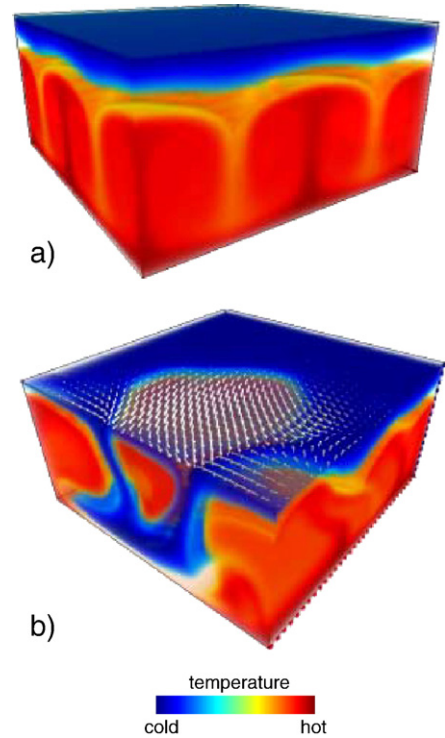


Fig. 2. Two snapshots of the colour-coded temperature field observed for the system shown in Fig. 1 (run 1) at different times: a) during the period of stagnant lid behaviour ( $t=1.0$ ) and b) during a mobilisation event ( $t=1.31$ ).

transition between different characteristic system states indeed occurs temporally for a fixed set of parameters. We have observed a system that initially shows the stagnant lid mode of convection but changes to a state in which episodic surface mobilisation occurs as time proceeds. Fig. 1 illustrates this temporal transition by means of the surface Nusselt number, i.e. the non-dimensional surface heat flux density. Initially, a low and temporally constant value of the Nusselt number is observed, identifying the stagnant lid mode of convection, while the heat flux is increased substantially during the individual episodes of surface mobilisation. Here, the lid that insulates the hot interior from the cold surface is subducted at least partially, thus allowing the hot upwellings to reach the surface, resulting in an elevated surface heat flux. Fig. 2 visualises the two different flow regimes. The colour-coded temperature fields are shown for the two time instants indicated in Fig. 1. The thick, immobile surface layer and the relatively hot interior which are characteristic for the stagnant lid regime [16] are clearly visible in Fig. 2a. The second snapshot (Fig. 2b) shows the temperature field during an event of surface mobilisation: about half the surface area is mobilised, with large patches of surface material moving

uniformly in the same direction as indicated by white velocity vectors. Material is subducted in the two downwellings at the front side of the model volume.

The temporal evolution of the Nusselt number (Fig. 1) indicates that the system shows stagnant lid convection for more than one thermal diffusion time. During this period the system is in a thermal equilibrium, the net flux of heat out of the system, which is shown in Fig. 3, is zero. Transient effects caused by the initial conditions have decayed after approx. 0.15 thermal diffusion times (cf. Fig. 3), hence the stagnant lid period is to be considered as an individual system state. The peculiarity of the system behaviour shown in Figs. 1, 2, and 3 is that it combines two different convective states in a single system, both individually lasting for a significantly long time. We therefore classify the observed system behaviour as being temporally transitional.

Apart from this prominent example for a transitional behaviour, we also observed systems that show stagnant lid convection being interrupted by isolated events of surface mobilisation. Fig. 4 illustrates such a situation, again by means of the surface Nusselt number.

Though the episodic regime produces a similar alternation between a mobilised and stagnant surface, the system behaviour shown in Fig. 4 is fundamentally different from that observed in the episodic regime: the individual events of surface mobilisation occur out of a quasi-steady state with an equilibrated heat budget, indicated by a temporally constant value of the Nusselt number in Fig. 4. This determining difference between the transitional behaviour and that observed for systems in the episodic regime is emphasised in Fig. 5 in which the surface Nusselt numbers for three different model runs are compared. The system in the episodic regime

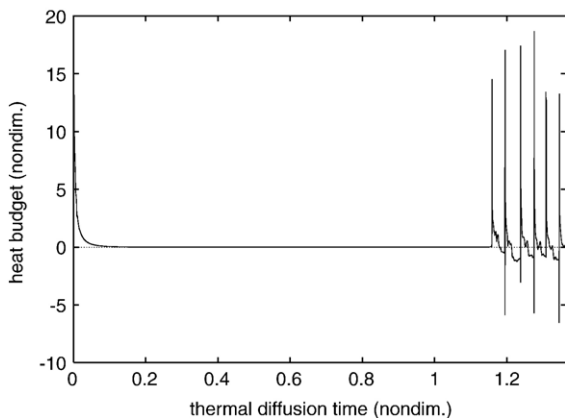


Fig. 3. Heat budget of the system that shows a transition from stagnant lid convection to an episodic behaviour (cf. Fig. 1) which is calculated as the sum of the surface and basal heat flux.

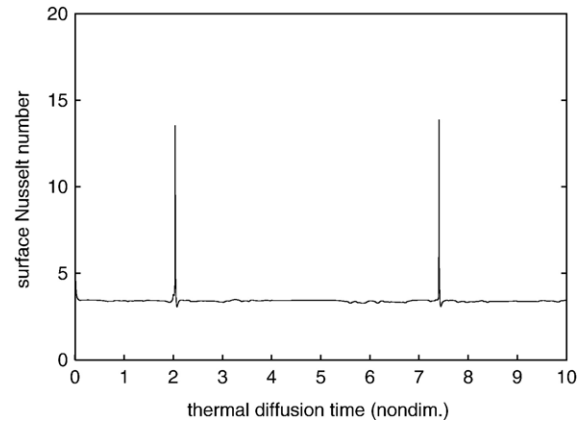


Fig. 4. Surface Nusselt number as a function of time for a system showing steady state stagnant lid convection interrupted by two isolated events of surface mobilisation at the times  $t=2.0$  and  $t=7.4$ . The temporally constant value of the Nusselt number indicates a thermally equilibrated system. For this calculation a Rayleigh number of  $Ra=100$  and a yield stress of  $\sigma_0=4.0$  have been applied (run 9).

(dashed line) exhibits a total of 13 mobilisation events during the time interval shown without returning to an equilibrated state between subsequent events. We therefore distinguish between the episodic regime and the transitional regime as observed in our calculations. On the other hand, the system behaviour observed in the transitional regime between two individual mobilisation events resembles that typical for the stagnant lid regime (cf. Fig. 5). The two regimes are hence virtually identical apart from the difference in the stability of the stagnant surface layer. It is, however, not possible to identify this difference and hence to predict the occurrence of further surface mobilisation events by means of first order observables like the temperature

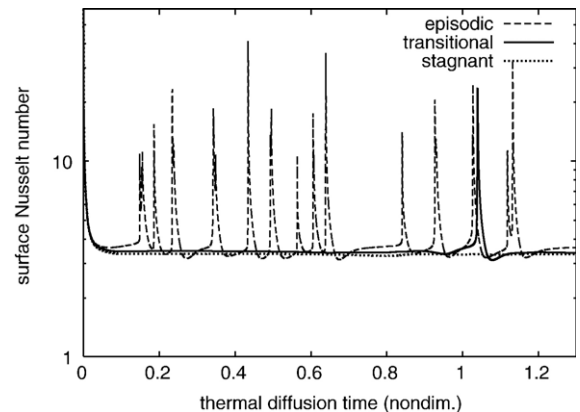


Fig. 5. Comparison of the different surface behaviours found in the stagnant lid, the transitional and the episodic regime. Shown is the surface Nusselt number as a function of time for the model calculations indicated as run 4, run 8 and run 14 in Table 1, respectively.

profile, the heat flux or the thickness of the stagnant lid for an individual system. We have therefore deduced a mobilisation criterion that does not only quantify the

stability of a stagnant surface layer but furthermore allows to predict whether further events of mobilisation will occur.

### 3.1. Mobilisation criterion

The individual convective regimes differ in surface behaviour and efficiency of heat transport and, consequently, also in their viscosity composition, as has been shown by Stein [24]. These findings are reviewed here since they provide the basis for the following quantitative analysis. The rheological law applied in our study (Eqs. (5) and (6)) leads to a viscosity that is controlled by the temperature-dependent part in the stagnant lid case while the influence of the strain-rate contribution prevails for a system in the mobile lid regime. The opposing viscosity compositions are illustrated in Fig. 6a and b, showing vertical profiles of the individual viscosity components ( $\eta_T$  and  $\eta_E$ ) and the effective viscosity  $\eta$ . The episodic regime (Fig. 6c) constitutes a particular regime. A stagnant lid-like surface behaviour is repeatedly interrupted by episodes of surface mobilisation. During the short phases of vanishing surface mobility the viscosity structure resembles that observed in the stagnant lid regime with a resulting viscosity that is controlled by the temperature-dependent part (cf. Fig. 6a). This dominance declines as the system approaches a mobilisation event. Within the (still immobile) lid, the viscosity finally reaches a configuration with balanced contributions of temperature and strain-rate just before the surface is mobilised. This is shown in Fig. 6c. Hence, in this situation the following expression holds for the surface layer:

$$\eta_T = \eta_E \quad (7)$$

Substituting the rheological law (Eq. (6)) and accounting for  $T=0$  at the surface yields

$$E/\sigma_0 = 1 \quad (8)$$

for the onset of surface mobilisation, where the plastic viscosity  $\eta^*$  has been neglected. We use this relation to define a mobilisation criterion:

$$\epsilon_M > 1 \quad (9)$$

where we introduced the mobilisation index

$$\epsilon_M := \left. \frac{E}{\sigma_0} \right|_{\text{surface}} \quad (10)$$

The mobilisation criterion given by Eq. (9) describes the stability of the system with respect to a mobilisation of the surface. The mobilisation index  $\epsilon_M$  is smaller than

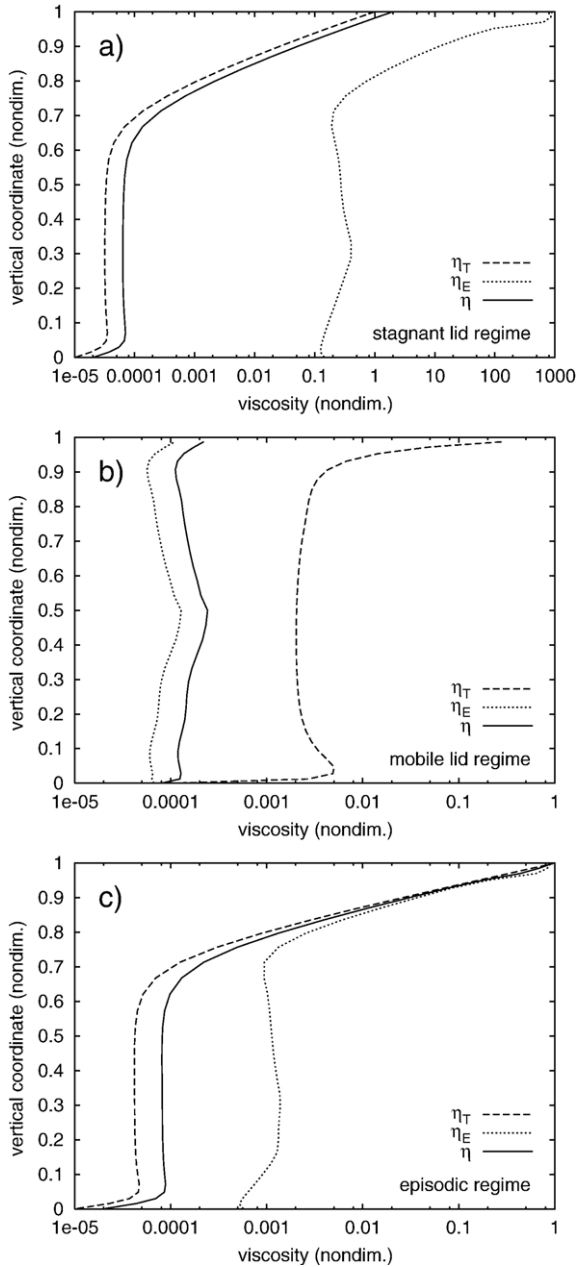


Fig. 6. Vertical profiles of the horizontally averaged value of the total viscosity  $\eta$  (solid line) and the individual contributions by temperature and strain-rate,  $\eta_T$  (dashed line) and  $\eta_E$  (dotted line), respectively. Shown are typical profiles for the stagnant lid regime (a, run 15), the mobile lid regime (b, run 0) and the episodic regime for a time instant just before the surface is mobilised (c, run 1). Note that the total viscosity is controlled by the smallest component due to the reciprocal summation in Eq. (5). The actual parameter values for the individual model runs are given in Table 1.

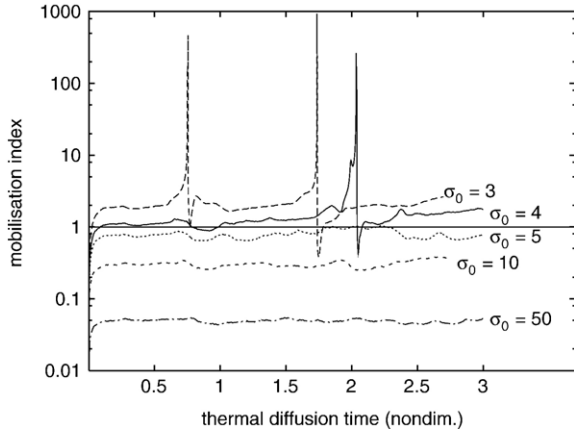


Fig. 7. Mobilisation index  $\epsilon_M$  as a function of time for model runs with a varying yield stress. Events of surface mobilisation are visible as temporally increased  $\epsilon_M$ . Mobilisation occurs only for runs with  $\sigma_0 \leq 4$ .

unity for a system which is in the stagnant lid regime and that therefore maintains an immobile surface.

### 3.2. Validation of the criterion

In order to validate the mobilisation criterion, we carried out a number of model calculations for parameter settings at the border between the stagnant lid and the episodic regime (cf. [20]). For a fixed Rayleigh number of  $Ra=100$  (defined at the surface) and a viscosity contrast of  $R=10^5$  we varied the yield stress  $\sigma_0$  between 2 and 200 thus covering both, the stagnant lid and the episodic regime and therefore also the range in which a transitional behaviour is to be expected. Purely basal heating ( $Q=0$ ) has been employed in all calculations. The calculations have been carried out in an aspect-ratio 2 box with a lateral and vertical resolution of 64 and 32 control volumes, respectively. In order to investigate the influence of the side walls, we carried out some calculations for an aspect ratio of  $4 \times 4 \times 1$  and found qualitatively the same behaviour as for the smaller aspect ratio. A vertical grid refinement at the upper and lower boundary has been applied in order to increase the spatial resolution within the thermal boundary layers.

The calculations with a yield stress of  $\sigma_0 \geq 5$  all show a stagnant lid behaviour while multiple events of surface mobilisation can be observed for runs with  $\sigma_0 \leq 3$ . The model calculation with  $\sigma_0=4$  shows a single mobilisation event followed by an extended phase of stagnant lid behaviour. The location of this boundary between the stagnant lid and the episodic regime has already been mapped by Stein et al. [20], however, these authors performed only a qualitative classification of the system

based on the surface behaviour finally emerging. Using the mobilisation index (Eq. (10)) we are moreover able to quantify the stability of the temporarily immobile surface layer. This allows a further differentiation of the intermittent system behaviour observed near the regime boundary and hence an analysis of the transitional behaviour shown in Figs. 1 and 4. Fig. 7 shows the mobilisation index  $\epsilon_M$  as a function of time for selected model runs. The figure reveals that our mobilisation criterion does indeed provide a possibility to quantify the stability of the conductive surface layer: Those model runs that yield values of the mobilisation index larger than unity, i.e. that fulfil the mobilisation criterion, show repeated mobilisation of the initially stagnant surface layer (cf.  $\sigma_0=3$ ) while for those with  $\epsilon_M$  smaller than one stagnant lid behaviour is exhibited throughout the time of observation ( $\sigma_0=5, 10$  and  $50$ ). The model run for  $\sigma_0=4$  (solid line in Fig. 7) illustrates the predictability of surface mobilisation events: A single event occurs at  $t=2.0$  followed by a long period of stagnant lid behaviour. During this stage the mobilisation index stays at a supercritical value of  $\epsilon_M \approx 1.7$  indicating that the system remains unstable against further surface mobilisation events. In fact, a second mobilisation occurs at  $t=7.3$  (not shown in Fig. 7 but cf. Fig. 4).

The results for a variation of the yield stress are summarised in Fig. 8, which shows the temporally averaged value of the mobilisation index  $\epsilon_M$  versus the applied yield stress  $\sigma_0$  for each model run. Systems that exhibit one or multiple events of surface mobilisation are indicated by small circles, while square symbols denote model runs in which the surface remains stagnant throughout time. The two types of convection (i.e. with

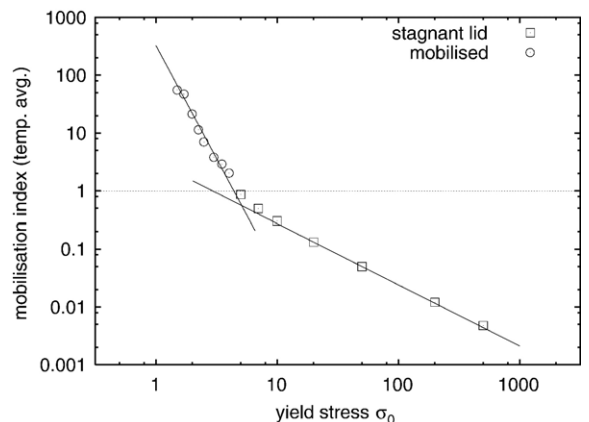


Fig. 8. Time-averaged value of the mobilisation index as obtained for different yield stresses. Circular symbols indicate systems that show events of surface mobilisation, whereas systems that remain in the stagnant lid regime are represented by small squares.

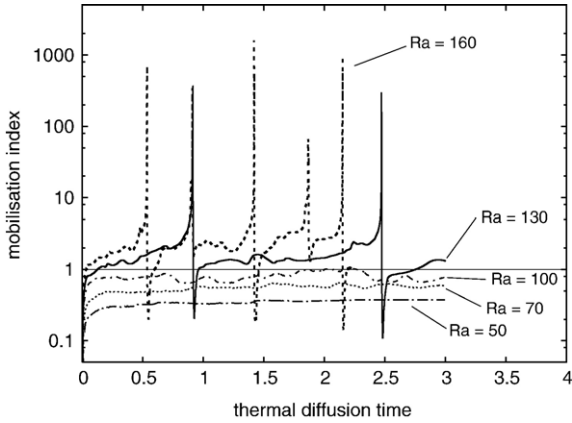


Fig. 9. Mobilisation index  $\epsilon_M$  as a function of time for selected model runs with varied Rayleigh number and constant yield stress (for  $\sigma_0=5.0$ ). Note that the number of mobilisation events per time increases for larger values of  $\epsilon_M$ .

and without sporadic surface mobilisation) are clearly separated by the critical value of  $\epsilon_M=1$ , as predicted by our mobilisation criterion. Different functional dependencies are observed for small and large values of the yield stress, respectively. We applied a power-law fit of the form  $f(\sigma_0)=a \cdot \sigma_0^b$  to the data for each of the two branches with the following results:

$$a = 327.0 \quad b = -3.91 \quad \text{for } \sigma_0 \leq 3.5 \quad (11)$$

$$a = 3.12 \quad b = -1.06 \quad \text{for } \sigma_0 \geq 10 \quad (12)$$

The second set of parameters (Eq. (12)) describes an almost reciprocal dependency of the mobilisation index

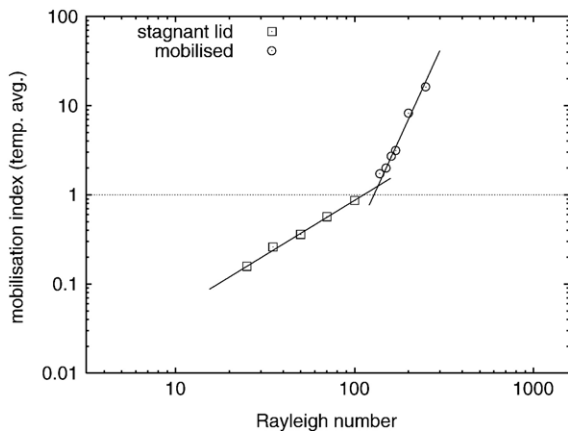


Fig. 10. Temporally averaged mobilisation index as a function of the Rayleigh number. Different symbols are used for model runs with and without surface mobilisation events. Solid lines indicate power-law fits to the data.

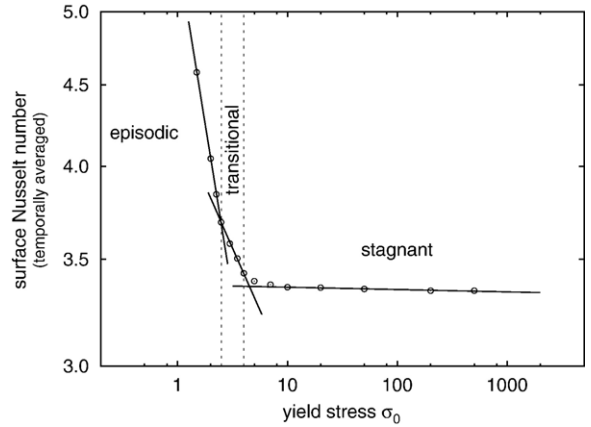


Fig. 11. Temporally averaged surface Nusselt number as a function of the applied yield stress. The solid lines represent three different power law fits to the data indicating three distinct regimes. Note the logarithmic scale on the ordinate axis.

on the yield stress, indicating that the effective strain-rate  $E$  has an only negligible influence on the mobilisation index for large values of  $\sigma_0$ .

In order to investigate the influence of the Rayleigh number on the value of the mobilisation index, we additionally carried out a series of model calculations for a fixed yield stress of  $\sigma_0=5.0$  and a Rayleigh number varied in the range of  $20 \leq Ra \leq 300$ , again covering all three, the stagnant lid, the transitional and the episodic regime. Fig. 9 shows the temporal evolution of the mobilisation index for selected model runs. Clearly, the results are in agreement with our mobilisation criterion (Eq. (9)). Mobilisation of the surface occurs only for systems with a mobilisation index  $\epsilon_M$  larger than unity. It should be mentioned that the mobilisation index may actually drop to values lower than unity even for systems which do show mobilisation events. This is, however, only a temporary effect caused by the reduced strain-rates within the moving surface layer. In such cases the mobilisation index immediately increases again until supercritical values are reached, as observed for a Rayleigh number of  $Ra=130$  (solid line in Fig. 9).

The time-averaged values of the mobilisation index for a variation of the Rayleigh number are shown in Fig. 10. Again, two different power-law relationships are found for asymptotically small and large values of the Rayleigh number, separated by the  $\epsilon_M=1$  threshold.

$$a = 3 \cdot 10^{-3} \quad b = 1.23 \quad \text{for } Ra \leq 100 \quad (13)$$

$$a = 5.5 \cdot 10^{-10} \quad b = 4.39 \quad \text{for } Ra \geq 130 \quad (14)$$

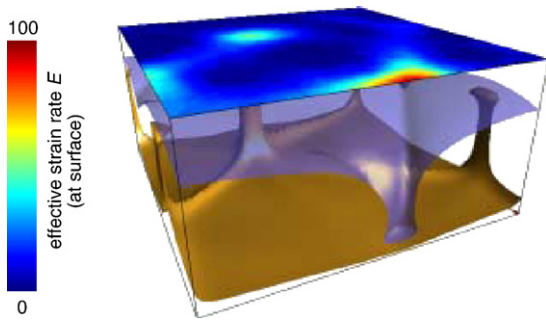


Fig. 12. Snapshot of a model calculation with  $Ra=150$  and  $\sigma_0=5.0$  (run 23) showing a colour-coded representation of the effective strain-rate in the top-most horizontal layer and two temperature isosurfaces for  $T=0.95$  and  $T=0.7$  in gold and transparent blue colour, respectively. Areas with elevated strain-rates are located directly above the large-scale up- and downward currents.

### 3.3. Difference to the episodic regime

Earlier in this section the difference between the episodic regime and the newly found temporally transitional regime has been defined in terms of the thermal state between two subsequent events of surface mobilisation: a system in the episodic regime does not reach a thermal equilibrium during this stage. While this definition is well suited for a coarse, relative description of the two regimes, it does not provide an absolute or quantitative distinction. Our studies, however, revealed a robust proof for the temporally transitional behaviour

constituting an individual regime fundamentally different from the episodic regime. Fig. 11 shows the temporally averaged value of the surface Nusselt number for a variation of the applied yield stress, i.e. for a parameter-induced change of the convective regime. The figure reveals that different  $Nu-\sigma_0$  scaling laws are not only found for the stagnant lid and episodic regime, but also for the transitional and the episodic regime, as indicated by the three power-law fits to the data. It is therefore reasonable to refer to the temporally transitional behaviour as an individual regime.

### 3.4. Trigger mechanisms

Those systems which fulfil the mobilisation criterion (Eq. (9)) can be considered as being unstable against surface mobilisation events. However, an unstable system may sustain an immobile surface layer for a finite period of time, as seen for the model run with  $\sigma_0=3$  in Fig. 7 which initially remains in the stagnant lid mode of convection for 0.7 thermal diffusion times. The duration of this supercritical stagnant lid phase generally depends on the value of the mobilisation index. Larger values of  $\epsilon_M$  result in systems that are mobilised more easily and typically after a shorter period of time (cf. the runs with  $\sigma_0=3$  and  $\sigma_0=4$  in Fig. 7 and the runs with  $Ra=130$  and  $Ra=160$  in Fig. 9).

The actual mobilisation of the surface of a supercritical system is triggered by locally elevated strain-rates within the stagnant lid: increased values of the strain-

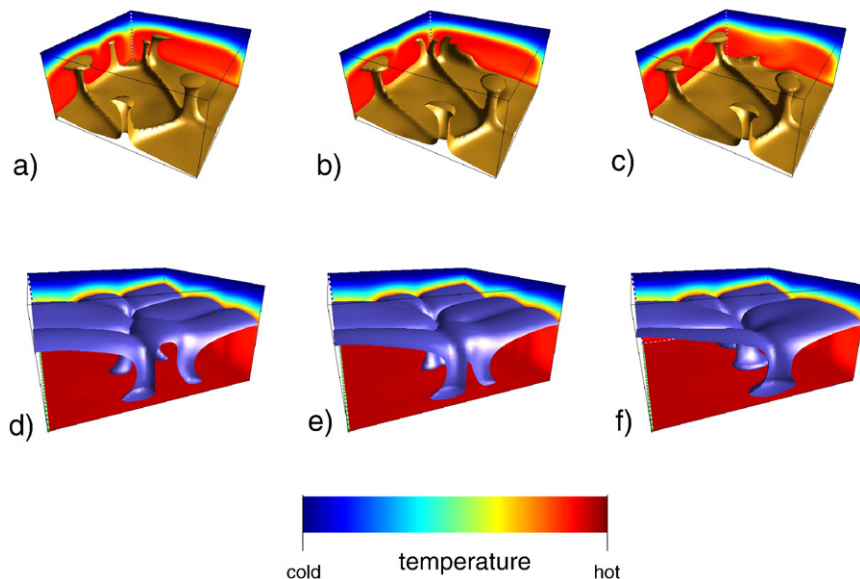


Fig. 13. Two series of snapshots of the temperature field showing the convergence and merging of upwellings (figures a–c, run 9) and downwellings (d–f, run 7), triggering a mobilisation event. The yellow and blue surfaces indicate a temperature of  $T=0.95$  and  $T=0.8$ , respectively. The sidewalls of the box show the temperature distribution at the corresponding boundaries according to the given colour-scale.

rate  $E$ , i.e. deformation results in a reduction of the viscosity (cf. Eq. (6)) in the affected area, thus allowing the otherwise stagnant surface to flow. Fig. 12 shows the distribution of the effective strain-rate in the surface layer for a system with a Rayleigh number of  $Ra=150$  and  $\sigma_0=5.0$  at a time instant directly before the surface is mobilised. The figure additionally illustrates the convective pattern by means of two temperature isosurfaces (for  $T=0.95$  and  $T=0.7$ ).

As the effective strain-rate is a function of the velocity field  $\mathbf{u}$ , the areas of increased strain-rates are associated with large-scale structures in the flow pattern as clearly visible in Fig. 12. Due to the time-dependent nature of the convective system, the up- and downwelling plumes that dominate the flow pattern are not stationary but are free to drift laterally. If two or more plumes collide, they typically merge and form a single, stronger up- or downwelling, exerting higher strain-rates to the overlying lid. Fig. 13 shows two series of snapshots of the temperature field illustrating this process. Three upwellings in the rear corner of the box, which are clearly discernible as separate structures in Fig. 13a, converge (Fig. 13b) and finally merge into a single upwelling plume (Fig. 13c) triggering the surface mobilisation. Fig. 13d–e show the corresponding process for two cold downstreams at the front side of the model domain.

#### 4. Conclusion

In our calculations we observed temporal variations in the convective style of the investigated systems for a fixed set of parameters: Stagnant lid convection is repeatedly interrupted by isolated events of surface mobilisation or

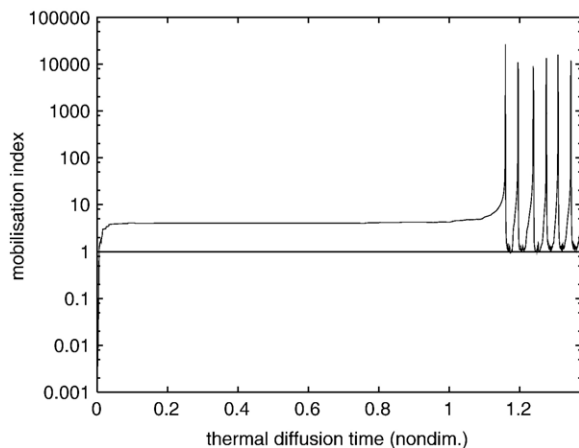


Fig. 14. Mobilisation index  $\epsilon_M$  as a function of time for the model run that shows a temporal transition from stagnant lid to episodic behaviour (cf. Fig. 1).

Table 1  
Summary of model runs presented in this paper

ID	$Ra$	$\sigma_0$	Regime	Figure
Run 0	100	0.1	Mobile	6
Run 1	100	1.0	Episodic	1–3, 6, 14
Run 2	100	1.5	Episodic	8
Run 3	100	1.7	Episodic	8
Run 4	100	2.0	Episodic	5, 8
Run 5	100	2.25	Transitional	8
Run 6	100	2.5	Transitional	8
Run 7	100	3.0	Transitional	7, 8, 13
Run 8	100	3.5	Transitional	5, 8
Run 9	100	4.0	Transitional	4, 7, 8, 13
Run 10	100	5	Stagnant	7, 8, 9
Run 11	100	7	Stagnant	8
Run 12	100	10	Stagnant	8
Run 13	100	20	Stagnant	8
Run 14	100	50	Stagnant	5, 7, 8
Run 15	100	200	Stagnant	6, 8
Run 16	100	500	Stagnant	8

Part 1: variation of the yield stress.

is, moreover, completely replaced by an episodic behaviour. In both cases the observed surface mobilisation occurs out of a thermally equilibrated system state identical to stagnant lid convection and can therefore not be explained as being the result of an initial transient period. Furthermore, the system returns to a thermally equilibrated state after the individual events of surface mobilisation which is not observed in the episodic regime. We therefore propose the existence of a further, temporally transitional regime located between the stagnant lid and the episodic regime. To further investigate this regime and to determine the difference to the stagnant lid regime, a large number of model calculations in the corresponding parameter range has been carried out. We deduced a mobilisation index in order to quantify the stability of the stagnant surface layer and the occurrence

Table 2  
Summary of model runs presented in this paper

ID	$Ra$	$\sigma_0$	Regime	Figure
Run 17	25	5.0	Stagnant	10
Run 18	35	5.0	Stagnant	10
Run 19	50	5.0	Stagnant	9, 10
Run 20	70	5.0	Stagnant	9, 10
Run 21	100	5.0	Stagnant	10
Run 22	130	5.0	Transitional	9, 10
Run 23	150	5.0	Transitional	10, 2
Run 24	160	5.0	Transitional	9, 10
Run 25	170	5.0	Transitional	10
Run 26	200	5.0	Episodic	10
Run 27	220	5.0	Episodic	10

Part 2: variation of the Rayleigh number.

of spontaneous surface mobilisation events. We also described a mechanism that triggers the mobilisation.

While the mobilisation criterion does not allow to forecast the exact time at which the surface is mobilised, it, however, does provide a necessary condition for the occurrence of a mobilisation event. At this point we therefore reconsider the system behaviour shown in Fig. 1, i.e. a temporal transition between stagnant lid and episodic regime, as the mobilisation criterion provides an interpretation of this behaviour. Fig. 14 shows the corresponding mobilisation index as a function of time, indicating that the critical value of  $\epsilon_M=1$  is already exceeded by a factor of four prior to the onset of episodic behaviour. The stagnant lid is thus extremely unstable with small fluctuations in the flow field being sufficient to trigger a mobilisation event.

The problem of a stagnant surface layer being mobilised has recently been investigated in [25]. In contrast to our work which aims at the fundamental description of the observed transitional behaviour, Solomatov [25] focused on the rheological effects of small-scale convection on the overlying plate. Despite the different focus of the two studies, the observed (dimensional) values for the critical yield stress of surface mobilisation are in good agreement: using Mars-like values for the reference viscosity, the mantle height and thermal diffusivity, we obtain a scaling constant for the (dimensionless) yield stress of roughly 2 GPa. Applying this scaling constant, the corresponding dimensional value resulting from our investigation is in the range of 5–25 GPa, which is of the same order of magnitude as the values found by Solomatov [25].

Temporal variations in the convective style and hence in the surface behaviour are of major interest for many planetological considerations. Our observations indicate that spontaneous changes in the surface behaviour are an inherent feature of the dynamics of a convective system, and may occur even out of a state of thermal equilibrium. This supports the theory, that the global, catastrophic resurfacing event assumed to have happened on Venus are of endogenous origin. Our results also demonstrate, that a short period of active plate tectonics followed by a stagnant lid behaviour as often speculated for Mars, is indeed dynamically plausible.

We are confident that our concept of a mobilisation index as a necessary criterion for the occurrence of surface mobilisation events is also useful for a further quantitative investigation of the episodic regime. We have in fact observed that for systems with a larger mobilisation index, the surface is mobilised more

frequently. Here, the different temporal characteristics ranging from a strictly periodic sequence of episodes to a fully irregular pattern await further exploration.

## Acknowledgement

A. Loddoch is supported by the Deutsche Forschungsgemeinschaft (DFG) — priority programme SPP 1115 “Mars and the terrestrial planets” under grant no. Ha 1765/10-3.

Some of the calculation presented in this work have been carried out using resources provided by the John-von-Neumann Institut for Computing, Jülich, Germany (project no. hms10).

## Appendix A. List of model runs

Tables 1 and 2 summarise all model runs presented in this paper along with the corresponding parameter settings. For all runs a viscosity contrast due to temperature of  $R=10^5$  has been assumed.

## References

- [1] C.C. Reese, V.S. Solomatov, L.-N. Moresi, Heat transport efficiency of stagnant lid convection with dislocation viscosity: application to Mars and Venus, *J. Geophys. Res.* 103 (1998) 13643–13657.
- [2] G. Choblet, C. Sotin, Early transient cooling of Mars, *Geophys. Res. Lett.* 28 (2001) 3035–3038.
- [3] D.L. Turcotte, An episodic hypothesis for Venusian tectonics, *J. Geophys. Res.* 98 (1993) 17061–17068.
- [4] R.G. Strom, G.G. Schaber, D.D. Dawson, The global resurfacing of Venus, *J. Geophys. Res.* 99 (1994) 10899–10926.
- [5] A.C. Fowler, S.B.G. O'Brien, A mechanism for episodic subduction on Venus, *J. Geophys. Res.* 101 (E2) (1996) 4755–4763.
- [6] C.C. Reese, V.S. Solomatov, L.-N. Moresi, Non-Newtonian stagnant lid convection and magmatic resurfacing of Venus, *Icarus* 139 (1999) 67–80.
- [7] N.H. Sleep, Martian plate tectonics, *J. Geophys. Res.* 99 (1994) 5639–5655.
- [8] F. Nimmo, D.J. Stevenson, Influence of early plate tectonics on the thermal evolution and magnetic field of Mars, *J. Geophys. Res.* 105 (2000) 11969–11979.
- [9] J.E.P. Connerney, M.H. Acuña, N.F. Ness, G. Kletetschka, D.L. Mitchell, R.P. Lin, H. Reme, From the cover: tectonic implications of Mars crustal magnetism, *Proc. Natl. Acad. Sci. U. S. A.* 102 (42) (2005) 14970–14975. URL <http://www.pnas.org/cgi/content/abstract/102/42/14970>.
- [10] K.C. Stengel, D.C. Oliver, J.R. Booker, Onset of convection in variable-viscosity fluid, *J. Fluid Mech.* 120 (1982) 411–431.
- [11] G. Schubert, Subsolidus convection in the mantles of terrestrial planets, *Annu. Rev. Earth Planet. Sci.* 7 (1979) 289–342.
- [12] G. Schubert, T. Spohn, Thermal history of Mars and the sulfur content of its core, *J. Geophys. Res.* 95 (1990) 14095–14104.
- [13] T. Spohn, Mantle differentiation and thermal evolution of Mars, Mercury, and Venus, *Icarus* 90 (2) (1991) 222–236.

- [14] J. Arkani-Hamed, On the thermal evolution of Mars, *J. Geophys. Res.* 99 (1994) 2019–2033.
- [15] O. Grasset, E.M. Parmentier, Thermal convection in a volumetrically heated, infinite prandtl number fluid with strongly temperature-dependent viscosity: implications for planetary thermal evolution, *J. Geophys. Res.* 103 (B8) (1998) 18171–18181.
- [16] V.S. Solomatov, Scaling of temperature-and stress-dependent viscosity convection, *Phys. Fluids* 7 (1995) 266–274.
- [17] D. Breuer, T. Spohn, Early plate tectonics versus single-plate tectonics on Mars: evidence from magnetic field history and crust evolution, *J. Geophys. Res.* 108 (2003) 5072.
- [18] L.N. Moresi, V.S. Solomatov, Mantle convection with a brittle lithosphere: thoughts on the global tectonic styles of the Earth and Venus, *Geophys. J. Int.* 133 (3) (1998) 669–682.
- [19] P.J. Tackley, Self-consistent generation of tectonic plates in time-dependent, three-dimensional mantle convection simulations, part 1: Pseudoplastic yielding, *Geochem. Geophys. Geosyst.* (2000) 1.
- [20] C. Stein, J. Schmalzl, U. Hansen, The effect of rheological parameters on plate behaviour in a self-consistent model of mantle convection, *Phys. Earth Planet. Int.* 142 (2004) 225–255.
- [21] M.T. Zuber, The crust and mantle of Mars, *Nature* 412 (2001) 220–227.
- [22] R.A. Trompert, U. Hansen, The application of a finite volume multi-grid method to three-dimensional flow problems in a highly viscous fluid with a variable viscosity, *Geophys. Astrophys. Fluid Dyn.* 83 (1996) 261–291.
- [23] S.A. Hauck, R.J. Phillips, Thermal and crustal evolution of Mars, *J. Geophys. Res.* 107 (6) (2002) 1–19.
- [24] Claudia Stein. *The effect of rheological parameters on plate-like features in a self-consistent mantle convection model*. PhD thesis, Universität Münster, 2005.
- [25] V.S. Solomatov, Initiation of subduction by small-scale convection, *J. Geophys. Res.* 109 (B01412) (2004). doi:10.1029/2003JB002628.